

# Statistical description of the shear-induced diffusion of a suspension of non-Brownian particles

I. Santamaría-Holek and G. Barrios

*Facultad de Ciencias, Universidad Nacional Autónoma de México,  
Circuito exterior de Ciudad Universitaria, 04510, D.F., México.*

J.M. Rubi

*Facultat de Física, Universitat de Barcelona,  
Av. Diagonal 647, 08028, Barcelona, Spain.*

Recibido el 21 de enero de 2009; aceptado el 13 de marzo de 2009

Using mesoscopic nonequilibrium thermodynamics, we calculate the entropy production of a dilute suspension of non-Brownian particles subject to an oscillatory shear flow. We find that an Onsager coupling leads to a breakdown of the fluctuation-dissipation theorem and to the shear induced diffusion effect observed in experiments. By contracting the description, we derive a Smoluchowski equation from which the scaling of the mean square displacement on the shear rate and particle diameter reported in experiments is obtained. We also perform lattice Boltzmann simulations to show the shear induced diffusion effects, and how the transition to irreversibility can be characterized through the power spectra of particle trajectories.

*Keywords:* Mesoscopic entropy; irreversibility; shear induced diffusion; lattice Boltzmann.

Usando la termodinámica de no equilibrio mesoscópica, calculamos la producción de entropía de una suspensión diluida de partículas no Brownianas sujetas a un flujo cortante oscilatorio. Encontramos que un acoplamiento de Onsager produce una violación del teorema de fluctuación disipación asociada a la difusión inducida por corte que ha sido observada previamente en experimentos. Al contraer la descripción, obtenemos la ecuación de Smoluchowski a partir de la cual se obtiene el desplazamiento cuadrático medio de las partículas. También realizamos simulaciones numéricas con el método de la ecuación de Boltzmann en redes mostrando que el flujo cortante oscilatorio induce efectos difusivos. La transición a la irreversibilidad puede ser caracterizada a través del espectro de potencia de la trayectoria de las partículas.

*Descriptores:* Entropía mesoscópica; irreversibilidad; difusión inducida por corte; ecuación de Boltzmann en redes.

PACS: 05.70.-a; 05.70.Ln

## 1. Introduction

In one of his challenging books, Prigogine discussed the idea that the non-integrability of the mechanical equations of motion of a system of particles is the cause of the irreversibility of their collective motion. Far beyond this idea, he proposed that the appropriate mathematical description of these non-integrable systems should be probabilistic [1].

In recent years, experiments performed with semi-diluted suspensions of spherical polymethylmethacrylate (PMMA) particles of diameter  $d \simeq 230\mu\text{m}$ , have shown that many body interactions are responsible for the transition from reversible to irreversible motion of non-Brownian particles suspended in a fluid [2]. In these experiments, the suspension is contained in a cylindrical Couette cell and is taken out of equilibrium by applying an oscillating shear flow  $\dot{\gamma} \cos(\omega t)$ , where  $\dot{\gamma} = \omega\gamma$  with  $\gamma_0$  the applied strain and  $\omega$  the characteristic frequency of the oscillation. At small enough Reynolds numbers it is observed that the motion of the particles is reversible, according to the classical result of hydrodynamics [5]. When increasing the Reynolds number the trajectories of the particles become chaotic and then their reversible behavior is lost.

The motion of the particles has been characterized through the mean square displacement (MSD) which scales

in the form:  $\langle \Delta x^2 \rangle \sim 2d^2\dot{\gamma}t$ . This result implies that the effective diffusivity scales with  $D \sim d^2\dot{\gamma}$ , giving rise to the so-called shear induced diffusion effect [2]. A statistical description has been offered in Ref. 6 by postulating a diffusion equation in which the diffusivities have been constructed by analyzing the temporal behavior of the correlation of the position of the particles. Although this approach makes it possible to use direct experimental measurements or simulation results in order to describe particular systems, it cannot offer a fundamental explanation of the shear induced diffusion effect.

In this article, we show that a general statistical description can be derived from more fundamental physics based on the second law of thermodynamics. Our theory leads to the same scaling of the MSD and effective diffusion coefficient as that found in experiments and may give an explanation of the transition to irreversibility since it takes into account the dependence of these quantities on the volume fraction occupied by the particles. In accordance with previous results, we show that the origin of the irreversibility is due to an Onsager coupling containing hydrodynamic interactions and leading to a breaking down of the fluctuation-dissipation relation.

The effect of the hydrodynamic interactions on the diffusion of a suspension of Brownian particles has been widely studied in the literature [11–15], and used to describe from

non-Newtonian effects [30] to jamming effects near the glass transition [14]. For suspensions under shear flow, a discussion of the breaking of the fluctuation-dissipation theorem has been found in previous works [8, 9, 18, 20, 23]. A similar result has been found for Brownian motion in rotating fluids [16]. The influence of external forces taking the system out of equilibrium and confinement is also connected with recent works on the existence and interpretation of macroscopic non-equilibrium parameters of states such as the temperature [17, 22, 24].

The article is organized as follows. In Sec. 2 we use non-equilibrium thermodynamics to formulate the mesoscopic model based on a Fokker-Planck equation. Section 3 is devoted to deriving a Smoluchowski equation and to obtain the effective diffusion tensor accounting for the shear-induced diffusion effect observed in experiments. In Sec. 4 we present Lattice-Boltzmann simulations characterizing the shear-induced diffusion effect via the power spectrum of particle movements affected by hydrodynamic interactions. Finally, in Sec. 5 we discuss our main results.

## 2. Fokker-Planck dynamics of a suspension under oscillatory flow

Consider a suspension of  $N$  spherical particles of radius  $a$  and mass  $m$  embedded in a Newtonian heat bath at constant temperature  $T$  and subjected to non-stationary nonequilibrium conditions imposed by the flow  $\vec{v}_0(\vec{r}, t)$ .

In order to describe the dynamics of this system, one may follow an effective medium approximation that takes into account hydrodynamic interactions in an effective form. In this approach, the description is carried out by means of the normalized single-particle probability distribution  $f(\vec{r}, \vec{u}, t)$  depending upon the instantaneous position  $\vec{r}$  and velocity  $\vec{u}$  of a test particle and time  $t$ . In the literature, it has been shown that the evolution in time of  $f$  is governed by the Fokker-Planck equation [8, 9]

$$\frac{\partial f}{\partial t} + \nabla \cdot (\vec{u}f) = \frac{\partial}{\partial \vec{u}} \cdot (f\vec{V}_{\vec{u}}), \quad (1)$$

where  $\nabla = \partial/\partial\vec{r}$  and the probability current in  $\vec{u}$ -space,  $f\vec{V}_{\vec{u}}$ , is given by

$$f\vec{V}_{\vec{u}} = -\vec{\beta} \cdot (\vec{u} - \vec{v}_0)f + \frac{k_B T}{m} \vec{\xi} \cdot \frac{\partial f}{\partial \vec{u}} - \vec{\zeta} \cdot \vec{F}f. \quad (2)$$

Here  $\vec{F} = d\vec{v}_0/dt$  and  $k_B$  is the Boltzmann constant. Equation (2) constitutes a linear law obtained after calculating the entropy production of the system and identifying forces and currents in the phase space of the system [10, 25]. This linear law introduces the Onsager coefficients  $\vec{\beta}$ ,  $\vec{\xi}$  and  $\vec{\zeta}$ . For simplicity in notation we have defined the coefficient  $\vec{\xi} = \vec{\beta} - \vec{\epsilon} \cdot \nabla \vec{v}_0$ . In Eq. (2),  $\vec{\beta}$  is the friction coefficient that usually appears when describing Brownian motion in velocity space [8, 9, 11] and corresponds to what is referred to as a direct effect in nonequilibrium thermodynamics [25]. The

coefficient  $\vec{\zeta}$  is related to inertial effects due to the change in time of  $\vec{v}_0$  whereas  $\vec{\epsilon}$  constitutes a cross effect relating the probability flows  $\vec{u}f$  and  $f\vec{V}_{\vec{u}}$  appearing in Eq. (1). This coupling term proportional to  $\vec{\epsilon}$  and  $\nabla \vec{v}_0$ , breaks down the fluctuation-dissipation relation between the drag and diffusion terms in Ref. 2, [8, 17, 24].

The expressions for  $\vec{\epsilon}$  and  $\vec{\zeta}$  have been obtained in Ref. 9 by using the generalized Faxén theorem giving the force experienced by a particle of arbitrary shape in a heat bath under non-stationary flow conditions [27]. For spherical particles at low Reynolds numbers one finds

$$\epsilon = \frac{1}{6} \frac{m}{k_B T} a^2 \beta_0^2 k_\omega, \quad (3)$$

where  $k_\omega = (1 + 2a\alpha_\omega + (59/45)a^2\alpha_\omega^2)$  and  $\zeta = \rho_p/\rho_f$  with  $\rho_p$  the density of the particle, and  $\rho_f$  the density of the host fluid.  $\alpha_\omega = \sqrt{-i\omega/\nu}$  is the inverse viscous penetration length of the host fluid and  $\nu$  its kinematic viscosity (see Refs. 9 and 27).

At intermediate and high volume fractions, hydrodynamic interactions become relevant since their magnitude depends on the relative position between particles  $\vec{r}_{ij} = \vec{r}_i - \vec{r}_j$ . These interactions introduce corrections to the mobility  $\vec{\mu}_{ij}$  of a particle and have been calculated by means of the induced force formalism [12]. These corrections depend on powers of the aspect ratios:  $a/r_{ij}$  and  $a/r_{ijs}$  with  $r_{ijs}$  the magnitude of the vector that points from sphere  $i$  to the mirror image with respect to a wall of sphere  $j$  [12].

We have previously mentioned that hydrodynamic interactions will be taken into account in an effective way through the form of the friction tensor  $\vec{\beta}$  or, equivalently, through the mobility tensor that in the lower order approximation we assume takes the form

$$\vec{\mu}_{ij} \simeq \beta_0^{-1} \vec{1} \delta_{ij} + \beta_0^{-1} \left[ \frac{3}{4} \frac{a}{r_{ij}} \left( \vec{1} + \hat{r}_{ij} \hat{r}_{ij} \right) (1 - \delta_{ij}) - \frac{3}{4} \frac{a}{r_{ijs}} \left( \vec{1} + \hat{r}_{ijs} \hat{r}_{ijs} \right) \right], \quad (4)$$

where  $\beta_0 = 6\pi\eta a/m$  is the Stokes friction coefficient per mass unit with  $\eta$  the viscosity of the host fluid. Here  $\hat{r}_{ij}$  and  $\hat{r}_{ijs}$  are the unit relative vectors between particles and between particle  $j$  and the wall. For  $i = j$ , Eq. (4) reduces to well known results for the mobility of a particle in the presence of a wall:  $\mu = \beta_0^{-1} (1 - B_1 a/l)$ , [28]. Here  $l$  is the distance of the particle to the wall and  $B_1$  may take different values depending on the direction of the motion of the particle with respect to the plane of the wall.

Equation (4) shows that hydrodynamic interactions introduce anisotropies depending on the aspect ratios:  $a/r_{ij}$  and  $a/r_{ijs}$ . In a first approximation, we shall assume that in our description the effective mobility taking into account the effects of hydrodynamic interactions can be represented through the tensor

$$\vec{\mu} = \beta_0^{-1} \left[ \vec{1} - \vec{g}(\phi) \right], \quad (5)$$

where  $\beta_\omega = \beta_0 (1 + a\alpha_\omega + (1/9)a^2\alpha_\omega^2)$  is a frequency dependent friction coefficient. The filling fraction  $\phi$  is related to an average distance  $r_{av}$  between particles. This quantity is related to the free volume in the system that the particles can visit. The minus sign takes into account the fact that diffusion decreases when the volume fraction grows ( $r_{av}$  decreases) [18, 19]. Thus, the unknown tensor  $\vec{g}$  contains on average the effects of hydrodynamic interactions on the particle. Notice that the friction and mobility coefficients satisfy the relation  $\vec{\beta} \cdot \vec{\mu} = \vec{1}$ .

It is convenient to stress here that a Fokker-Planck equation similar to Eqs. (1) and (2) has been derived in Ref. 23 by following the methods of the kinetic theory of gases. In particular, the authors obtained that the correction of the coefficient in the diffusion term depends on the viscous part of the pressure tensor of the host fluid.

### 3. The Smoluchowski equation and the origin of irreversibility

In order to discuss the origin of the irreversibility it is convenient to analyze the long-time regime of the system occurring at times  $t \gg \beta_{ij}$ . In this regime, the description can be performed in terms of the evolution equation for the reduced probability density

$$\rho(\vec{r}, t) = \int f(\vec{r}, \vec{u}, t) d\vec{u}. \quad (6)$$

To obtain the mentioned equation we must first derive the evolution equations for the first three moments of  $f$  defined by Eq. (6) and

$$\rho\vec{v}(\vec{r}, t) = \int \vec{u} f d\vec{u}$$

and

$$\vec{P}^k(\vec{r}, t) = \int (\vec{v} - \vec{u})(\vec{v} - \vec{u}) f d\vec{u}.$$

Taking the time derivative of these definitions, using Eqs. (1) and (2) and integrating by parts, one obtains the following evolution equation for the zero-order moment [8, 9]:

$$\frac{\partial \rho}{\partial t} = -\nabla \cdot (\rho\vec{v}). \quad (7)$$

For the first order moment  $\rho\vec{v}$  one finds

$$\rho \frac{d\vec{v}}{dt} + \nabla \cdot \vec{P}^k = -\rho\vec{\beta} \cdot (\vec{v} - \vec{v}_0) + \rho\vec{\zeta} \cdot \vec{F}, \quad (8)$$

whereas the evolution equation for the second moment is

$$\frac{d}{dt} \vec{P}^k + 2 \left( \vec{P}^k \cdot \vec{\tau}^{-1} \right)^s = \frac{2k_B T}{m} \rho \vec{\xi}^s. \quad (9)$$

The upper symbol  $s$  means the symmetric part of a tensor and the matrix of relaxation times  $\vec{\tau}$  is defined by

$$\vec{\tau} = \left[ \vec{\beta} + \nabla\vec{v} + \frac{1}{2}(\nabla \cdot \vec{v})\vec{1} \right]^{-1}. \quad (10)$$

Equations (7)-(9) pertain to a time ordered hierarchy of equations in which we have neglected the contributions arising from higher order moments since they relax much faster than those involved in (7)-(9), [8].

For the low Reynolds-number linear flows typical of the experiments of interest to us, one may derive the following long-time ( $t \gg \tau_{ij} \simeq \beta_{ij}^{-1}$ ) expressions for the second moment:

$$\vec{P}^k \simeq \frac{k_B T}{m} \rho \vec{1} - \frac{k_B T}{m} \rho \left( \vec{\mu} + \epsilon \vec{\mu} \cdot \nabla \vec{v}_0 \right)^s, \quad (11)$$

and the first moment

$$\rho\vec{v} \simeq \rho\vec{v}_0 + \rho\zeta\vec{\mu} \cdot \vec{F} - \vec{\mu} \cdot \left( \nabla \cdot \vec{P}^k \right), \quad (12)$$

where we have used the relation between  $\vec{\mu}$  and  $\vec{\beta}$  and, in writing (11), used the approximation  $\vec{v} \approx \vec{v}_0 + O(\nabla \ln \rho)$ . Substituting Eq. (11) into (12) and the resulting expression into (7) we finally obtain the Smoluchowski equation [8]

$$\frac{\partial \rho}{\partial t} = -\nabla \cdot \left( \rho\vec{v}_0 + \zeta\vec{\mu} \cdot \vec{F} \right) + \nabla \cdot \left( \vec{D} \cdot \nabla \rho \right), \quad (13)$$

where after using (4) we have defined the *effective diffusion coefficient*

$$\vec{D} = \frac{k_B T}{m} \vec{\mu} \cdot \left( \vec{1} - \vec{\mu} \cdot \nabla \vec{v}_0 \right)^s - \frac{1}{6} a^2 \beta_0^2 k_\omega \vec{\mu} \cdot \left( \vec{\mu} \cdot \nabla \vec{v}_0 \right)^s. \quad (14)$$

This coefficient contains two contributions; one depending on the temperature and one contribution independent of it. Therefore, the first terms are related to Brownian motion whereas the last one is related to non-thermal effects. This last term accounts for the linear scaling on the shear rate and time of the mean square displacement when the system is subjected to oscillatory flow conditions.

Equation (13) can also be derived from the mesoscopic nonequilibrium formalism by approaching the problem through an N-particle theory [29]. In this case, instead of the one particle distribution function  $f$ , one uses the N-particle distribution function  $P^{(N)}(\{\vec{r}\}^N, \{\vec{u}\}^N, t)$  depending on the positions ( $\{\vec{r}\}^N$ ) and velocities ( $\{\vec{u}\}^N$ ) of the N-particles. The mesoscopic thermodynamic approach leads to the multivariate Fokker-Planck equation [29]

$$\begin{aligned} \frac{\partial P^{(N)}}{\partial t} + \sum_{i=1}^N \nabla_{\vec{r}_i} \cdot (\vec{u}_i P^{(N)}) &= \sum_{i,j=1}^N \frac{\partial}{\partial \vec{u}_i} \\ &\cdot \left\{ \left[ (\vec{u}_i - \vec{v}_i^0) \cdot \vec{\beta}_{ij} - \vec{\zeta}_{ij} \cdot \vec{F}_i \right] P^{(N)} \right. \\ &\left. + \frac{k_B T}{m} \vec{\xi}_{ij} \cdot \frac{\partial P^{(N)}}{\partial \vec{u}_i} \right\}, \end{aligned} \quad (15)$$

where the subindexes  $i$  and  $j$  refer to different particles and the tensors  $\vec{\beta}_{ij}$ ,  $\vec{\zeta}_{ij}$  and  $\vec{\xi}_{ij}$  have the same physical interpretation as their one particle counterparts but explicitly containing hydrodynamic interactions as given by Eq. (4). In particular one obtains  $\vec{\xi}_{ij} = \vec{\beta}_{ij} - \vec{\epsilon}_{ij} \cdot \nabla \vec{v}_i^0$ , where the term  $\nabla \vec{v}_i^0$  indicates that the velocity gradient must be evaluated at the position of the  $i$ -th particle. The definitions of the other quantities are the same as in the case of Eq. (2).

In the long time limit  $t \gg \beta_0^{-1}$ , the mesoscopic description given through Eq. (15) can be reduced to a diffusion description in terms of a multivariate Smoluchowski equation in which the diffusion coefficient is of the form (14). However, in this case it is possible to show that the effective mobility tensor is, in general, a function of the position, time and the filling fraction  $\phi$ ,  $\vec{\mu}(\vec{r}, t; \phi)$ , [29].

### 3.1. Shear induced diffusion

Let us assume now that the flow imposed on the system is a shear flow in the  $x$  direction, *i.e.*,  $\vec{v}_0(\vec{r}, t) = \vec{r} \cdot \vec{\gamma}$  with  $\gamma_{21} = \dot{\gamma} \cos(\omega t)$  and zero otherwise. The shear rate is related to the applied strain  $\gamma_0$  by  $\dot{\gamma} = \gamma_0 \omega$ . For the sake of simplicity, we shall neglect inertial effects related to  $\zeta$ .

The MSD of the particle can be calculated by taking the time derivative of the definition

$$\langle r^2 \rangle = \int (x^2 + y^2) \rho d\vec{r}, \quad (16)$$

where we are considering the two dimensional case due to the symmetry of the problem and for simplicity in the presentation. Let us substitute Eq. (13) now into the result. An integration by parts leads to

$$\frac{d}{dt} \langle r^2 \rangle = 2\dot{\gamma} \cos(\omega t) \langle xy \rangle(t) + 2Tr[\vec{D}], \quad (17)$$

where  $\langle xy \rangle(t) = \int xy \rho d\vec{r}$ . Similarly, we must derive the evolution equations for  $\langle xy \rangle(t)$ ,  $\langle x^2 \rangle(t)$  and  $\langle y^2 \rangle(t)$ . After solving the obtained set of differential equations, for low shear rates and frequencies ( $\dot{\gamma} < 1$ ,  $\omega < 1$ ), we may expand the MSD as a power series on  $\dot{\gamma}$  and  $\omega$  in order to obtain

$$\langle r^2 \rangle \simeq \left\{ 2D_0[3 - g_{11}(\phi) - g_{22}(\phi)] + \frac{1}{3}g_{12}(\phi)d^2\dot{\gamma} \right\} t - 2D_0g_{12}(\phi)d^2\dot{\gamma}t^2, \quad (18)$$

where  $d = 2a$  and we have assumed  $g_{12} = g_{21}$  for simplicity and make explicit the dependence of  $g_{ij}$  on the volume fraction. For sufficiently large particles one may assume that  $D_0 \ll d^2g_{12}(\phi)\dot{\gamma}$  and then obtain the relation

$$\langle r^2 \rangle \sim \frac{1}{3}g_{12}(\phi)d^2\dot{\gamma}t. \quad (19)$$

When Eq. (19) is expressed in terms of the number  $n$  of cycles,  $t = 2\pi n/\omega$ , it gives:  $\langle r^2 \rangle \sim (2\pi/3)g_{12}(\phi)d^2\dot{\gamma}_0n$ ,

which has the same scaling relation for the mean square displacement as that reported in the experiments [2]. It is interesting to notice that, at low shear rates and frequencies, Eq. (18) suggests that the external forcing induces an *effective temperature*  $T_{eff}/T_0 = 1 + 2d^2g_{12}(\phi)\dot{\gamma}/D_0$ . Physically this means that the applied shear modifies the energy available to the particle in order to perform its shear induced diffusion.

An important difference between Eq. (19) and the scaling relations previously obtained from theoretical grounds (see, for instance, Ref. 6) is the coefficient  $g_{12}(\phi)$  due to hydrodynamic interactions. The dependence on the volume fraction may explain the transition to irreversibility as observed in the experiments [2]. Therefore, by starting from the second law of thermodynamics, our theory predicts that hydrodynamic interactions are responsible for the shear-induced diffusion effect and the transition to irreversibility through the dependence of the coefficients  $g_{ij}$  on  $(\phi)$ . The results we have obtained coincide with those emerging from the analysis of the dynamics of transition from reversible to irreversible behaviors.

## 4. Lattice-Boltzmann simulations

The threshold to irreversibility can also be studied by means of numerical simulations. This study is necessary to prove that the statistical description followed here and that based on the analysis of the dynamics of particles trajectories coincides. In order to characterize the shear-induced diffusion effect and the transition to the irreversibility, we shall use the lattice-Boltzmann method since it is based on a kinetic equation that does not contain thermal noise effects.

In particular, we shall use the  $D2Q9$  model for the lattice Boltzmann method with the BGK approximation [33, 34]. In this model, space is discretized in a two dimensional square lattice with nine velocities ( $\mathbf{c}_i$ ,  $i = 0 \dots 8$ ) allowed. The particle distribution functions  $f(\mathbf{r}, t)$ , at site  $r$  and time  $t$ , evolve according to the lattice Boltzmann equation

$$f_i(\mathbf{r} + \Delta t \mathbf{c}_i, t + \Delta t) - f_i(\mathbf{r}, t) = -\frac{\Delta t}{\tau} \left[ f_i(\mathbf{r}, t) - f_i^{(eq)}(\mathbf{r}, t) \right], \quad (20)$$

where  $\tau$  is the dimensionless relaxation time related to viscosity and  $f_i^{(eq)}$  are the local equilibrium distribution functions,

$$f_i^{(eq)} = w_i \rho \left[ 1 + 3\mathbf{c}_i \cdot \mathbf{u} + \frac{9}{2}(\mathbf{c}_i \cdot \mathbf{u})^2 - \frac{3}{2}u^2 \right]. \quad (21)$$

In this equation  $w_i=4/9$ ,  $1/9$ ,  $1/36$  are the weights associated with the lattice [35] for each set of velocities  $|\mathbf{c}_i| = 0, 1, \sqrt{2}$  and  $\rho$  and  $\mathbf{u}$  are the density and velocity defined by

$$\rho(\mathbf{r}, t) = \sum_i f_i(\mathbf{r}, t), \quad \mathbf{u}(\mathbf{r}, t) = \frac{1}{\rho} \sum_i f_i(\mathbf{r}, t) \mathbf{c}_i. \quad (22)$$

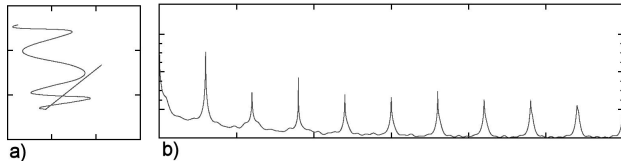


FIGURE 1. (a) Trajectory and (b) power spectrum of the  $x$ -trajectory of one particle for  $Re = 0.01$ ,  $\phi = 0.14$  and  $f^* = 10.0$ .

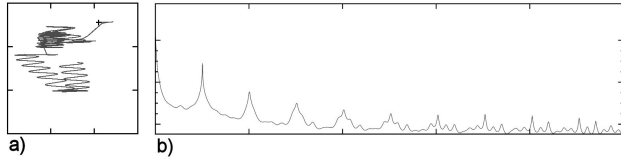


FIGURE 2. (a) Trajectory and (b) power spectrum of the  $x$ -trajectory of one particle for  $Re = 0.07$ ,  $\phi = 0.14$  and  $f^* = 10.0$ .

The viscosity is related to the dimensionless relaxation time by  $\nu = c_s^2(\tau - 1/2)$ , where  $c_s = 1/\sqrt{3}$  is the speed of sound in the  $D2Q9$  model.

The no-slip boundary conditions are simulated on the solid particles and the torques and forces are also evaluated to update the particles position at all times [36]. The particles' interactions are implemented with the method proposed by Ladd [37] and with the corrections made by Aidun *et al* [36]. The walls of the cavity use the bounce-back boundary condition, which consists in reversing the incoming particle distribution function after the stream process.

#### 4.1. Dimensionless numbers and numerical simulations

The problem can be characterized by three dimensionless numbers. The first one is the Reynolds number

$$Re = \frac{U_o H}{\nu}, \quad (23)$$

where  $U_o \cos \omega t$  is the velocity of the upper wall,  $H$  the height of the cavity,  $\nu$  the viscosity of the fluid,  $t$  the time and  $\omega$  the angular frequency. The second dimensionless number is the volume fraction occupied by the particles inside the cavity

$$\phi = \frac{N \pi r^2}{WH}, \quad (24)$$

where  $N$  is the number of particles,  $r$  the radius and  $W$  the width of the cavity. Finally, the third number is the dimensionless frequency given by

$$f^* = \frac{\omega}{2\pi\gamma}, \quad (25)$$

where  $\omega = 2\pi f$  is the angular frequency,  $f$  the frequency and  $\gamma = U_o/H$  the shear rate. The time is scaled with the period  $t^* = t/\tau$  and the position and lengths with the radius of the particle  $(x^*, y^*) = (x/r, y/r)$ .

The numerical simulations are carried out in a cavity of  $H^* = 11.33$  and  $W^* = 44.66$ . The relaxation time and the radius of the particles are kept constant in all simulation at

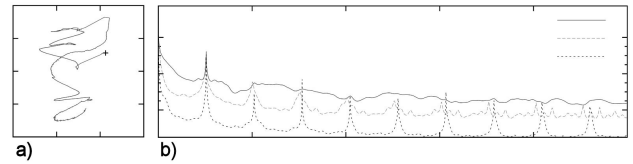


FIGURE 3. (a) Trajectory and (b) power spectrum of the  $x$ -trajectory of one particle for  $Re = 0.08$  and the two previous power spectra corresponding to the last two figures and  $\phi = 0.14$  and  $f^* = 10.0$ .

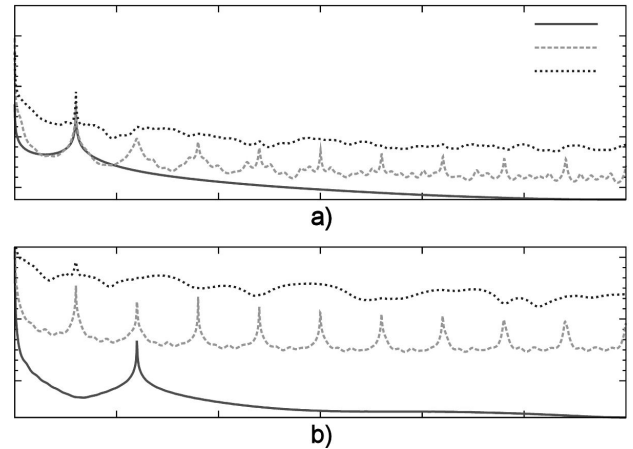


FIGURE 4. Power spectrum of the mean square displacement for (a)  $x$  and (b)  $y$  and  $Re = 0.08$  and different values of the particle concentration.

$\tau = 20.0$  and  $r = 4.5$ . We varied the Reynolds number ( $Re$ ), the volume fraction of particles  $\phi$ .

The diffusion of the particles can be increased by increasing the particle concentration  $\phi$  or by increasing the Reynolds number, even at small values of the  $Re$ . As an example, in Fig. 1 we present the trajectory of one of the sixteen particles and the power spectrum of the  $x$  movement. As can be appreciated in Fig. 1a the particle describes a regular movement and even though in Fig. 1b we can notice some harmonics, result of the hydrodynamic interactions between all particles, the motion can be described as regular.

When increasing the Reynolds number to  $Re = 0.07$ , the trajectory of the particle changes considerably as can be seen from Fig. 2a; also, the power spectrum shown in Fig. 2b changes, new subharmonics appear and the energy of each peak is smaller than the previous power spectrum shown, thus showing how the energy is distributed more homogeneously in many modes.

Finally, when  $Re = 0.08$  the particles exhibit a very irregular movement as shown in Fig. 3a; this can also be appreciated from the  $PS$  shown in Fig. 3b, where the only peak corresponds to the source of the oscillatory flow and now the other modes are gone due to the strength of the hydrodynamic particle interactions. In Fig. 3b we have added the  $PS$  of the two previous figures in order to make a visual comparison of the modes contained in the trajectories.

To obtain more evidence of the hydrodynamic interactions we kept  $Re = 0.08$  and varied the concentration of particles  $\phi$  as can be seen from Fig. 4, where we present the PS for the (a)  $x$  and (b)  $y$  msd. When the concentration is low there is only one peak for both the  $x$  and  $y$  msd, showing a weak coupling for the  $y$  msd. When increasing the concentration of particles the harmonics start to appear and grow. For the highest values of the particle concentration the peaks of the harmonics almost disappear and the energy is distributed along all the frequencies.

## 5. Discussion

In this paper we have explained the origin of the chaotic (irreversible) motion of a semi-diluted suspension of particles under the action of oscillating shear and extensional flows.

By analyzing the problem in phase space through the methods of the mesoscopic nonequilibrium thermodynamics, we conclude that the origin of the irreversibility is due to three factors:

- a) Hydrodynamic interaction between particles,
- b) finite-size effects and
- c) the violation of the fluctuation-dissipation theorem due to the imposed flow.

Lattice-Boltzmann simulations were performed to reinforce the theoretical results, indicating that the threshold to irreversibility can be characterized through the power spectra of the trajectories of the particles.

Our theory shows that the appropriate analysis of the entropy production at the mesoscale gives a thermodynamic explanation of the transition to irreversibility and the shear-induced diffusion effect. This explanation leads to the same results as those obtained from the theory of dynamical systems.

## Acknowledgments

ISH and GBV wish to acknowledge financial support by DGAPA-UNAM under grant IN-102609.

- 
1. I. Prigogine, *Les lois du chaos* (Flammarion, Paris, 1993).
  2. D.J. Pine, J.P. Gollub, J.F. Brady, and A.M. Leshansky, *Nature* **438** (2005) 997.
  3. D. Drazer, J. Koplik, B. Khusid, and A. Acrivos, *J. Fluid Mech.* **460** (2002) 307.
  4. V. Breedveld, D. van den Ende, A. Tripathi, and A. Acrivos, *J. Fluid Mech.* **375** (1998) 297.
  5. G.I. Taylor and J. Friedman, *Low Reynolds Number Flows* (National Committee on Fluid Mechanics Films, Encyclopedia Britannica Educational Corp., United States, 1996).
  6. A. Seriou and J.F. Brady, *J. Fluid Mech.* **506** (2004) 285.
  7. G. Boffeta, M. Cencini, M. Falcioni, and A. Vulpiani, *Phys. Rep.* **356** (2002) 367.
  8. I. Santamaría-Holek, D. Reguera, and J. M. Rubi, *Phys. Rev. E* **63** (2001) 051106.
  9. I. Santamaría-Holek, J.M. Rubi, A. Pérez-Madrid, *New J. Phys.* **7** (2005) 35.
  10. D. Reguera, J.M. G. Vilar, and J.M. Rubi, *J. Phys. Chem. B* **109** (2005) 21502.
  11. R. Zwanzig, *Adv. Chem. Phys.* **15** (1969) 325.
  12. W.V. Saarloos and P. Mazur, *Physica A* **120** (1983) 77; *Physica A* **127** (1984) 451.
  13. M. López de Haro, J.M. Rubi, *J. Chem. Phys.* **88** (1987) 1248.
  14. L. Yeomans-Reyna, H. Acuña-Campa, and M. Medina-Noyola, *Phys. Rev. E* **62** (2000) 3395.
  15. J.M. Rubi and P. Mazur, *Physica A* **250** (1998) 253.
  16. G. Ryskin, *Phys. Rev. Lett.* **61** (1988) 01442.
  17. R. Mauri and D. Leporini, *Europhys. Lett.* **76** (2006) 1022.
  18. S. Sarman, D.J. Evans, and A. Baranyai, *Phys. Rev. E* **46** (1992) 893.
  19. C.I. Mendoza and I. Santamaría-Holek, **130** (2009) 044904.
  20. Y. Drossinos and M.W. Reeks, *Phys. Rev. E* **71** (2005) 031113.
  21. G. Subramanian and J.F. Brady, *Physica A* **334** (2004) 343.
  22. A.V. Popov and R. Hernandez, *J. Chem. Phys.* **126** (2007) 244506.
  23. R. Rodríguez, E. Salinas-Rodríguez, and J. Dufty, *J. Stat. Phys.* **32** (1983) 279.
  24. J.V. Sengers and J.M. Ortíz de Zárate, *J. Non-Equilib. Thermodyn.* **32** (2007) 319.
  25. S.R. de Groot and P. Mazur, *Non-equilibrium Thermodynamics* (Dover, New York, 1984).
  26. J.W. Dufty and J.M. Rubi, *Phys. Rev. A* **36** (1987) 222.
  27. P. Mazur and D. Bedeaux, *Physica A* **76** (1974) 235.
  28. J. Happel and H. Brenner, *Low Reynolds number hydrodynamics* (Kluwer Academic Publishers, Dordrecht, 1991).
  29. I. Santamaría-Holek, G. Barrios, and J.M. Rubi, *Phys. Rev. E* **79** (2009) 031201.
  30. G. Bossis and J.F. Brady, *J. Chem. Phys.* **91** (1989) 1866.
  31. K.F. Freed and M. Muthukumar, *J. Chem. Phys.* **69** (1978) 2657.
  32. M. Mayorga, L. Romero-Salazar, and J.M. Rubi, *Physica A* **307** (2002) 297.

33. Y. Qian, D. d'Humieres, and P. Lallemand, *Eur. Phys. Lett.* **17** (1992) 479.
34. P.L. Bhatnagar, E.P. Gross, and M. Krook, *Phys. Rev.* **94** (1954) 511.
35. X. He and L.S. Luo, *Phys. Rev. E* **56** (1997) 6811.
36. C.K. Aidun, Y. Lu, and E.J. Ding, *J. Fluid Mech.* **373** 287 (1998).
37. A.J.C. Ladd, *J. Fluid Mech.* **271** (1994) 285; A.J.C. Ladd, *J. Fluid Mech.* **271** (1994) 311.